Study on laser-generated Lamb waves propagation in viscoelastic and anisotropic plate

Hongxiang Sun (孙宏祥), Baiqiang Xu (许伯强)*, Guidong Xu (徐桂东), and Chenguang Xu (徐晨光)

Faculty of Science, Jiangsu University, Zhenjiang 212013, China

**E-mail: bqxu@ujs.edu.cn*

Received March 23, 2010

The propagation characteristics of laser-generated Lamb waves in thin composite plates are theoretically studied. Taking the anisotropic and viscoelastic properties of the composite material into account, the finite element models for simulating laser-generated Lamb waves in the composite material are established in the frequency domain. Numerical results are calculated in purely elastic and viscoelastic transversely isotropic plates, respectively. The effects of the anisotropic and viscoelastic properties on the propagation of Lamb waves are analyzed in detail. The numerical results exhibit that the features of the laser-generated Lamb wave, including attenuation, velocity, frequency, and the dispersive nature, have a close relationship with the anisotropic and viscoelastic properties of the material.

OCIS codes: 140.3460, 310.2790.

doi: 10.3788/COL20100808.0776.

Laser ultrasound technique (LUT)[1−3] is a promising technique for nondestructive evaluation and material characterization applications because of its noncontact feature and its ability to generate broadband signals. For this reason, previous studies have investigated the wave propagation using this technique, such as bulk waves[4], surface acoustic waves[5,6], and even Lamb waves in thin plates[7,8]. However, the numerous publications regarding this subject offer limited information, as they are mainly concerned with modeling only elastic materials. Given that polymers or polymer-based matrix composites are widely used in aircraft, spacecraft, and other engineering industries, and because these materials possess anisotropic and viscoelastic properties that can strongly affect the propagation of ultrasonic waves, the LUT in the application of nondestructive evaluation of composite materials has attracted increasing attention in recent years.

Laser-generated ultrasonic waves in anisotropic and viscoelastic structures, which are generally encountered in aeronautical materials and micro-electro-mechanical systems (MEMSs), are of considerable interest because of their application in the nondestructive evaluation of anisotropic and viscoelastic properties. In order to determine the properties of a given composite material, the signal generated by a laser source in such a material must be well understood. Nevertheless, the features of the generated ultrasound are dependent on the anisotropy and the viscoelasticity in the composite material. Hence, the signals will become difficult to interpret. Many publications can be found so far in the propagation of laser ultrasonic waves in anisotropic materials, but the viscoelasticity of materials was ignored[9−13]. To date, little work has been published on the investigation of laser-generated ultrasound problems in viscoelastic and anisotropic solids. Constitutive relations developed in the Fourier domain have been modeled, using complex moduli representing the viscoelastic material properties that allow the dynamic behavior of these media to be properly described as well as several cases of the propagation of ultrasonic waves in plates made of dissipative materials[14,15]. However, these models are limited to investigating viscoelastic waves generated by various transducers that cannot obtain ultrasound signals with high spatial resolution.

Due to the complexity of the generation and propagation of laser ultrasonic waves in viscoelastic and anisotropic materials, numerical methods are more suitable in dealing with complicated processes, especially those that involve various parameters. The finite element (FE) method[16,17], used in solving problems in the frequency domain[18,19], has many advantages. It is flexible in terms of modeling complicated geometries and can easily obtain full field numerical solutions. In addition, compared with the classical FE method[12,13] utilizing numerical routines requiring hundreds or thousands of iterative calculations to produce time marching solutions, the proposed method is more time-efficient; this is because it consists of solving the dynamic equations of equilibrium for a limited number of frequencies that constitute the frequency spectrum of a temporal excitation. Furthermore, the complex moduli representing the viscoelastic property introduced in this method can effectively simulate the propagation of laser ultrasonic waves in viscoelastic materials. In this letter, the FE method is adopted to establish the models of laser-generated Lamb waves in composite plates in the frequency domain. Laser-generated Lamb waves in anisotropic and viscoelastic plates are also studied quantitatively.

An infinite homogeneous transversely isotropic plate made of a linearly viscoelastic material with thickness h was considered (Fig. 1). Coordinates x, y, and z of the model were chosen to be parallel with the principal axis of the medium, with y being the optical axis of the pulsed laser line source radiation. The motion was assumed to take place in three dimensions (x, y, and z), and the displacements in the x, y, and z directions are represented as u, v, and w, respectively. Here, the pulsed laser line source extended along a given direction and produced non-null displacements in both directions of x and y only (Fig. 2). With the plain strain conditions

$\varepsilon_{xz} = \varepsilon_{yz} = \varepsilon_{zz} = 0$, the displacement w and all derivatives with respect to z vanished. The displacement of the two-dimensional (2D) general equation is written in the frequency domain as[19]

$$\begin{cases} C_{11}^{*}\widetilde{u}_{xx} + C_{12}^{*}\widetilde{v}_{xy} + C_{66}^{*}(\widetilde{u}_{yy} + \widetilde{v}_{xy}) + \rho\omega^2\widetilde{u} = 0 \\ C_{22}^{*}\widetilde{v}_{yy} + C_{12}^{*}\widetilde{u}_{xy} + C_{66}^{*}(\widetilde{u}_{xy} + \widetilde{v}_{xx}) + \rho\omega^2\widetilde{v} = 0 \end{cases}, \quad (1)$$

where $(\widetilde{u}, \widetilde{v})$ is the Fourier transform of the displacement vector, ρ is the material density, and ω is the angular frequency. The moduli C_{ij}^{*} in Eq. (1) can be defined to be complex quantities if the material is viscoelastic: $C_{ij}^{*} = C_{ij}^{'} + \mathrm{i}C_{ij}^{''}$, with the real and imaginary parts representing the elastic and viscoelastic moduli, respectively. The aforementioned partial differential equation (Eq. (1)) must be written in the following form imposed by the commercial software used in this study[20]:

$$\nabla \cdot (c\nabla\widetilde{U}) - a\widetilde{U} = 0, \quad (2)$$

where ∇ is the vector differential operator defined as $\nabla = \left(\frac{\partial}{\partial x}, \frac{\partial}{\partial y}\right)$; the $\widetilde{U}$ to be determined corresponds to the displacement vector $(\widetilde{u}, \widetilde{v})$; the coefficients c and a are 2×2 matrices[19].

The boundary conditions are expressed as the Neumann type, which corresponds to an excitation source on the laser illuminative region and to a stress-free boundary on the others. In addition, the initial displacement and velocity are null.

Equations (1) and (2) are valid in any plane, where x and y represent the orthotropic axis of the plane of propagation. The composite plate made of unidirectional fibers has the transverse isotropy symmetry. The viscoelastic moduli are defined in a coordinate system, where the y direction is normal to the plate, the z direction coincides with the fibers, and the x direction is normal to fibers (Fig. 1). If the pulsed laser line source extends along z and produces non-null displacements in both directions x and y, the plane of propagation is isotropic and $C_{22}^{*} = C_{11}^{*}$, $C_{12}^{*} = C_{11}^{*} - 2C_{66}^{*}$. On the other hand, if the pulsed laser line source extends along x and produces non-null displacements in both directions y and z only, the plane of propagation is anisotropic and the previous moduli in Eqs. (1) and (2) are replaced as follows: C_{11}^{*} by C_{33}^{*}, C_{66}^{*} by C_{55}^{*}, and C_{12}^{*} by C_{13}^{*}.

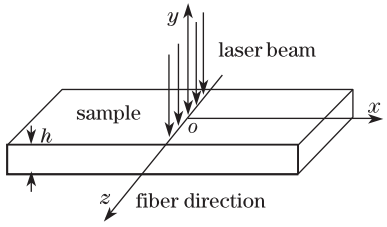

Fig. 1. Schematic diagram for laser irradiating sample.

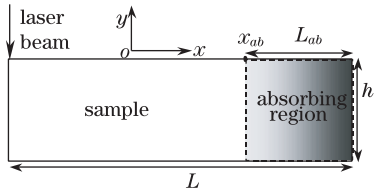

Fig. 2. Cross-section of the sample.

When modeling the propagation in the frequency domain, viscoelastic absorbing regions (ARs) must be used around the plate to avoid undesired reflections that would exist due to the permanent established regime (Fig. 2). In 2D problems, these regions consist of areas having gradually increasing viscoelastic properties, so that incoming waves do not encounter extreme changes in the acoustic impedance while being increasingly attenuated as they propagate deeply into the AR. The following function is used to define complex moduli involved in the AR[21]:

$$\mathrm{Im}(C_{ij}^{*\mathrm{AR}}) = C_{ij}^{''} + A(\frac{|x_{ab} - x|}{L_{ab}})^3 C_{ij}^{'}, L - L_{ab} < x \le L, \quad (3)$$

where $C_{ij}^{'}$ and $C_{ij}^{''}$ represent the material properties in the domain of propagation (DP), i.e., the domain of interest for the generation and propagation; $C_{ij}^{*\mathrm{AR}}$ represents the material properties in the AR; $x_{ab} = 30$ mm is the position of the interface separating the DP and the AR; $L = 40$ mm is the length of the plate; $L_{ab} = 10$ mm is the length of the AR; and $A = 50$ is a coefficient that may be adjusted to minimize the acoustic impedance mismatch between the DP and the AR.

The spatial resolution of the FE model is critical for the convergence of these numerical results. The spatial mesh of the plate is defined so that the smallest wavelength of any mode is supposed to propagate in the frequency range of the excitation. Triangular elements with quadratic behavior are used to mesh the DP, which satisfies[18]:

$$L_e \le \frac{1}{10}\frac{C}{f_{\max}}, \quad (4)$$

where L_e is the length of the mesh, C represents the highest (longitudinal) wave speed of the medium, and $f_{\max}$ is the highest frequency in the ultrasonic fields.

The numerical example illustrated in this letter is for the plate made of carbon fibers impregnated in an epoxy matrix. The material is anisotropic and viscoelastic, and has been widely used in the aerospace industry. Typical material properties used as input data in the calculation are given in Table 1[22].

Harmonic waves can be generated by using pulsed laser techniques[23]. In this letter, the laser source is replaced by an equivalent stress and is given by[24]

$$f(t) = \frac{2}{\alpha\sqrt{2\pi}} \exp\left[-\frac{(t - t_0)^2}{2\alpha^2}\omega_c^2\right] \sin(\omega_c t), \quad (5)$$

Table 1. Complex Viscoelastic Properties of the Carbon Fibers/Epoxy Matrix Composite Material

Density ρ(g/cm^3)	1.82
C_{11}^{*}(GPa)	12+0.8i
C_{33}^{*}(GPa)	140+10i
C_{66}^{*}(GPa)	3.3+0.2i
C_{55}^{*}(GPa)	6.2+0.4i
C_{13}^{*}(GPa)	6+0.9i

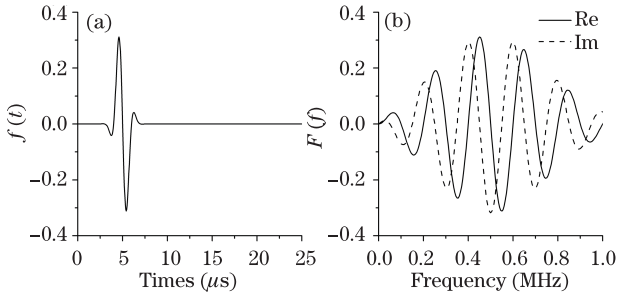

Fig. 3. (a) Time history of the excitation signal and (b) its frequency spectrum.

where α is a parameter controlling the pulse width, t_0 determines the pulse delay time, and $\omega_c = 2\pi f_c$ is the center angular frequency of the pulse. Here, we choose $\alpha = 1.2$, $t_0 = 5$ μs, and $f_c = 0.5$ MHz. Figures 3(a) and (b) show the time history of the chosen excitation pulse and its frequency spectrum, $f(t)$ and $F(f)$, respectively.

The frequency spectrum $F(f)$ is typically used as the excitation source of the FE model in the frequency domain. As shown in Fig. 3(b), the frequency content of the pulse is confined to $0 \leq f \leq 1$ MHz, and 100 frequency components are enough to represent the excitation source. In the calculation, 100 stationary analysis runs for the corresponding forces amplitudes were performed using the single parametric solution in the frequency domain. Complex displacements were then predicted in both x and y directions for the whole set of nodes. Temporal waveforms were reconstructed for several node positions by applying an inverse Fourier transform for the set of complex displacements that were predicted for the 100 frequency components of the input.

In the 2D model, the plane is supposed to be 40 mm in length and 0.1 mm in thickness, and the position of the laser source is located at $x = 0$, as shown in Fig. 2. Two distinct cases were hereby investigated. In the first case, the carbon fibers/epoxy matrix composite material was considered to be a purely elastic material (except for the AR). The real elastic modulus shown in Table 1 was used as input data. Afterwards, a viscoelastic material was considered, in which a complex viscoelastic modulus was used as input data.

Figures 4(a) and (b) show the normal displacement waveforms propagating along the x and z directions in the plate, respectively. The source-receiver distances are 3 and 6 mm, respectively. The shapes of the viscoelastic waveforms look very similar to those in purely elastic medium. It is shown that the propagation velocities of the viscoelastic waves are the same as those of the elastic waves. This is because the viscoelasticity of the material has no effect on the propagation velocity of ultrasonic waves. Moreover, the result shows that the lower frequency components of the symmetric mode (s_0) and asymmetric mode (a_0) are dominant in such a thin plate. At early times, the mode s_0 arrives at the observation point first, followed later by the dispersive mode a_0. The amplitude of the mode s_0 is less than that of the mode a_0. In addition, the mode s_0 exhibits a non-dispersive spike, while the dispersive nature of the mode a_0 is clear, i.e., the high-frequency components of the mode a_0 travel faster than the lower frequency components.

Many distinctions can be found when comparing the transient waveforms in Figs. 4(a) and (b). For instance, the velocities of the modes s_0 and a_0 propagating along the z direction are faster than those propagating along the x direction. This is because the real elastic modulus along the fiber direction is larger than what is considered normal to the fiber direction. In addition, Fig. 4 shows that the material viscoelasticity has no effect on the dispersion of the mode a_0. However, the mode a_0 propagating along the x direction shows a clearer dispersive nature than that propagating along the z direction. This phenomenon is also shown in Fig. 5. Furthermore, the frequencies of the mode a_0 propagating along the x direction are higher than those propagating along the z direction. Numerical results obtained by the FE method are compared with the experimental results reported before[11]. In the case of the anisotropic plate, finding good agreement in terms of the characteristics of the modes s_0 and a_0 propagation is imperative.

Comparing the transient waveforms in the viscoelastic material with those in the purely elastic material, viscoelasticity is clearly shown to have a significant influence on the features of laser-generated Lamb waves.

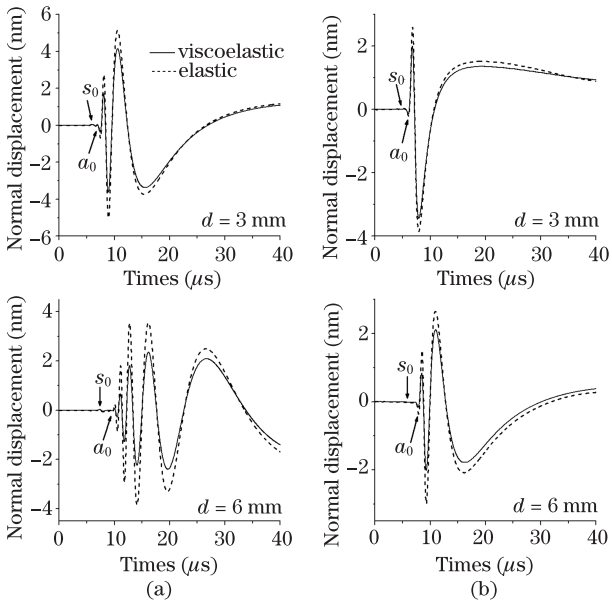

Fig. 4. Transient viscoelastic and elastic waveforms in the 0.1-mm-thick carbon fibers/epoxy matrix plates. (a) Along x direction; (b) along z direction.

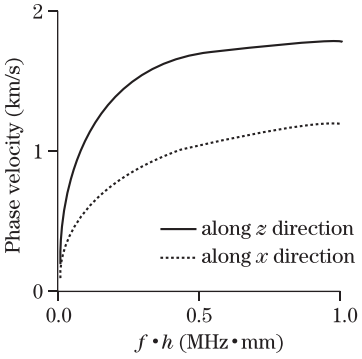

Fig. 5. Dispersion curves of the mode a_0 in the 0.1-mm-thick viscoelastic carbon fibers/epoxy matrix plate.

Figure 4 shows that the amplitudes of the elastic waves are significantly higher than those of the viscoelastic waves. This is particularly true for the mode a_0, which is more sensitive to the material viscoelasticity than the mode s_0. The amplitude ratio of the mode a_0 of the viscoelastic wave to the elastic wave decreases with the increase of the source-receiver distance in the same propagating direction, demonstrating the effect of the linear viscoelasticity of the material. Moreover, the amplitudes of the higher-frequency components of the mode a_0 significantly vary more than the lower-frequency ones, as shown in Fig. 4. This is because the attenuation in higher-frequency modes is generally higher than that in the lower-frequency modes.

Figure 6 shows the huge effect of viscoelasticity on the amplitudes of the s_0 and a_0 modes coexisting at the frequencies ranging from 0.2 to 0.8 MHz. The Lamb mode amplitude decreases gradually in the DP, i.e., from $x = 0$ to 30 mm, and is minute when entering the AR if the material viscoelasticity is taken into account. As expected, in the AR, i.e., from $x = 30$ to 40 mm, the amplitude drastically diminishes and tends toward zero, indicating that no wave propagates backwards along the DP to influence the incident wave. It is also shown in Fig. 6 that the amplitudes of the higher-frequency components of the Lamb mode significantly vary more than the lower-frequency ones, which is in agreement with the numerical results presented in Fig. 4.

In conclusion, the propagation of laser-generated Lamb waves in composite plates have been studied quantitatively by employing the FE method in the frequency domain, taking into account the anisotropic and viscoelastic properties of the material. Numerical results show the laser-generated ultrasonic waves in a thin plate are typical Lamb waves. The amplitudes of the viscoelastic Lamb waves decrease gradually with the increase of the propagation distance; in addition, the attenuation of various frequency components of the Lamb wave are also different. The waveforms propagating in the direction normal to the fiber exhibit clearer dispersive characteristics of the Lamb wave signal, and the frequencies are higher than the waveforms propagating in the direction parallel to the fiber direction. These results play an important role in conducting nondestructive evaluation and characterization of the sheet composite materials in the industry.

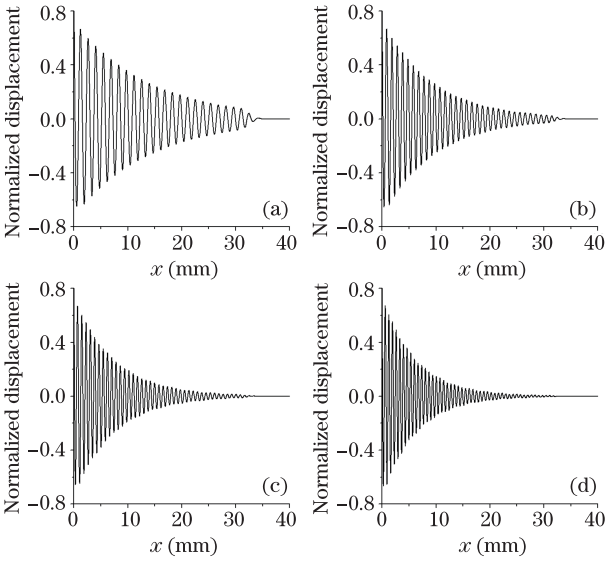

Fig. 6. Surface normalized normal displacement along the x direction at different frequencies of (a) 0.2, (b) 0.4, (c) 0.6, and (d) 0.8 MHz in the viscoelastic plate.

This work was supported by the Natural Science Foundation of the Jiangsu Higher Education Institutions of China under Grant No. 08KJB140003.

References

1. S. Zhang, Applied Acoustics (in Chinese) **11,** (4) 1 (1992).
2. Y. Shi, Z. Shen, X. Ni, and J. Lu, Chinese J. Lasers (in Chinese) **35,** 1627 (2008).
3. X. Chen, Acta Opt. Sin. (in Chinese) **29,** 203 (2009).
4. F. A. McDonald, Appl. Phys. Lett. **56,** 230 (1990).
5. L. Yuan, X. Ren, G. Yan, Z. Shen, X. Ni, J. Lu, and Y. Zhang, Chinese J. Lasers (in Chinese) **35,** 120 (2008).
6. L. Yuan, G. Yan, Z. Shen, H. Xu, X. Ni, and J. Lu, Chin. Opt. Lett. **6,** 837 (2008).
7. J. C. Cheng and S. Y. Zhang, Appl. Phys. Lett. **74,** 2087 (1999).
8. Z. Shen, B. Xu, X. Ni, and J. Lu, Chinese J. Lasers (in Chinese) **31,** 1275 (2004).
9. M. Dubois, F. Enguehard, L. Bertrand, M. Choquet, and J.-P. Monchalin, Appl. Phys. Lett. **64,** 554 (1994).
10. D. H. Hurley and J. B. Spicer, J. Appl. Phys. **86,** 3423 (1999).
11. T.-T. Wu and Y.-H. Liu, Ultrasonics **37,** 405 (1999).
12. B. Xu, J. Feng, G. Xu, J. Wang, H. Sun, and G. Cao, Appl. Phys. A **91,** 173 (2008).
13. B. Xu, F. Wang, J. Feng, J. Wang, H. Sun, and Y. Luo, Sci. China Ser. E Tech. Sci. **52,** 566 (2009).
14. C. W. Chan and P. Cawley, J. Acoust. Soc. Am. **104,** 874 (1998).
15. M. Castaings and B. Hosten, J. Acoust. Soc. Am. **113,** 2622 (2003).
16. J. Liu, S. Sun, and Y. Guan, Chinese J. Lasers (in Chinese) **35,** 276 (2008).
17. H. Ding, M. Huang, Y. Tong, Z. Li, S. Xie, and W. Gong, Acta Opt. Sin. (in Chinese) **28,** 1983 (2008).
18. H.-X. Sun, B.-Q. Xu, J.-J. Wang, G.-D. Xu, C.-G. Xu, and F. Wang, Acta Phys. Sin. (in Chinese) **58,** 6344 (2009).
19. H. Sun and B. Xu, Chinese J. Lasers (in Chinese) **37,** 537 (2010).
20. COMSOL AB, "COMSOL multiphysics user's guide, version 3.4" http://www.comsol.com/ (May 2008).
21. B. Hosten and M. Castaings, J. Acoust. Soc. Am. **117,** 1108 (2005).
22. B. Hosten and M. Castaings, NDT&E International **39,** 195 (2006).
23. C. M. Hernandez, T. W. Murray, and S. Krishnaswamy, Appl. Phys. Lett. **80,** 691 (2002).
24. O. M. Mukdadi and S. K. Datta, "Transient ultrasonic guided waves in bi-layered anisotropic plates with rectangular cross section" in D. O. Thompson and D. E. Chimenti, (eds.) *Review of Quantitative Nondestructive Evaluation* (Vol. 23) (American Institute of Physics, New York, 2004) p.238.